Theor Appl Climatol (2017) 130:945–958
DOI 10.1007/s00704-016-1928-1

ORIGINAL PAPER

Spatial and temporal trends of reference crop evapotranspiration and its influential variables in Yangtze River Delta, eastern China

Yu Xu[1] · Youpeng Xu[1] · Yuefeng Wang[1] · Lei Wu[1] · Guang Li[1] · Song Song[1]

Received: 28 January 2016 / Accepted: 2 September 2016 / Published online: 14 September 2016

Abstract Reference crop evapotranspiration (ETo) is one of the most important links in hydrologic circulation and greatly affects regional agricultural production and water resource management. Its variation has drawn more and more attention in the context of global warming. We used the Penman-Monteith method of the Food and Agriculture Organization, based on meteorological factors such as air temperature, sunshine duration, wind speed, and relative humidity to calculate the ETo over 46 meteorological stations located in the Yangtze River Delta, eastern China, from 1957 to 2014. The spatial distributions and temporal trends in ETo were analyzed based on the modified Mann-Kendall trend test and linear regression method, while ArcGIS software was employed to produce the distribution maps. The multiple stepwise regression method was applied in the analysis of the meteorological variable time series to identify the causes of any observed trends in ETo. The results indicated that annual ETo showed an obvious spatial pattern of higher values in the north than in the south. Annual increasing trends were found at 34 meteorological stations (73.91 % of the total), which were mainly located in the southeast. Among them, 12 (26.09 % of the total) stations showed significant trends. We saw a dominance of increasing trends in the monthly ETo except for January, February, and August. The high value zone of monthly ETo appeared in the northwest from February to June, mid-south area from July to August, and southeast coastal area from September to January. The research period was divided into two stages—stage I (1957–1989) and stage II (1990–2014)—to investigate the long-term temporal ETo variation. In stage I, almost 85 % of the total stations experienced decreasing trends, while more than half of the meteorological stations showed significant increasing trends in annual ETo during stage II except in February and September. Relative humidity, wind speed, and sunshine duration were identified as the most dominant meteorological variables influencing annual ETo changes. The results are expected to assist water resource managers and policy makers in making better planning decisions in the research region.

✉ Youpeng Xu
xypnju@163.com

Yu Xu
xuyu906@163.com

[1] School of Geographic and Oceanographic Sciences, Nanjing University, Nanjing, China

1 Introduction

It is widely accepted that climate has changed greatly due to natural factors and human activities in the last few decades. Some of the researchers have already shown great devotion to the study of spatial and temporal characterization of meteorological factors (Tayanc et al. 1997; Zhang et al. 2001; Lins and Slack 2005; Sahoo and Smith 2009; Chi et al. 2013). The topic that we are concerned with here includes not only the detecting of isolated temperature or precipitation but the effects caused by climate change on potential evapotranspiration. As it is restricted by a large number of variables, such as meteorological factors, soil types, and vegetation ratios, accurate regional evapotranspiration assessment borders on the impossible. Reference crop evapotranspiration (ETo) is frequently used to calculate accurate evapotranspiration. Evapotranspiration is one of the most important parameters in the earth surface hydrological cycle and plays a key role in estimating and predicting the water requirements of agricultural production, regional water resource management, and related policymaking. Generally speaking, assessment of

ETo variability can be helpful in regional sustainable development, especially in arid, semiarid, and climatic transitional areas. Moreover, discussion about the driving factors is always essential, because ETo is affected by geomorphology and climatic factors such as temperature, wind speed, sunshine duration, and relative air humidity (Thomas 2000; Jhajharia et al. 2009).

Through decades of sustained development, numerous equations for estimating ETo emerged (e.g., Penman 1948; Thornthwaite 1948; Blaney et al. 1950; Monteith 1965; Priestley and Taylor 1972; FAO-56 Penman-Monteith equation, 1998). Among those methods, the Penman-Monteith equation has been accepted as it incorporates both energy balance and aerodynamic theory. In the context of global warming, studies in recent years have suggested that ETo decreased over the past several years in many parts of the world, such as the USA (Lawrimore and Peterson 2000; Burn and Hesch 2007), Australia (Roderick et al. 2007; Jones et al. 2009), India (Bandyopadhayay et al. 2009), South Korea (Nam et al. 2015), and Iran (Dinpashoh et al. 2011). Similar phenomena have also been found in most parts of China (Yang et al. 2009; Zhang et al. 2010; Feng et al. 2014; Shan et al. 2015; Zhao et al. 2014; Chen et al. 2015). The main reasons involve the decrease in sunshine duration, radiation, and wind speed, and the increase of relative humidity. Apart from that, increasing trends in ETo have also been detected in many other regions, such as northern Northeast China, Central China, and parts of South China (Yin et al. 2010), Romania (Croitoru et al. 2013), and southeast and northeast Iran (Dinpashoh et al. 2011). In addition, the ETo in most of those regions experienced strong decadal variability. Mostly, the temporal patterns showed higher ETo values before the 1970s and a decrease until the 1990s, and since the 1990s, an increasing trend became dominant again. The ETo changes are the integrated consequences of numerous factors, such as climatic factors, air pollution, plant types, and urbanization.

It should be noted that papers addressing the topic of ETo have already been published (Xu et al. 2006; Zhang et al. 2011a, 2011b, 2015). They have discussed the spatial and temporal patterns of ETo and expounded the natural and human factors in parts of China. However, the researches have been mostly focused on the different climate types, administrative districts, and large river basins. But such contents might not be able to fully mirror the ETo behavior in the climatic transitional zones in the Yangtze River Delta (YRD), eastern China. Since the water resources are managed at a provincial scale, three provinces and one municipality located in East China are selected as the research areas. The middle and north region, one of the most important rice and winter wheat production areas, is vulnerable since the area experiences a transitional climate from humid to semiarid and has large water resource demand for agricultural and industrial production. At the same time, demands for drinking water and industrial and agricultural production, are always challenged by hot summer in the mid-south.

Therefore, the objectives of the present study are (1) to fully understand the spatial patterns of annual and monthly ETo in the research area from 1957 to 2014 based on the Penman-Monteith method, (2) to detect the temporal changes of annual and monthly ETo with Trend-Free Pre-Whitening (TFPW) Mann-Kendall trend test and the wavelet analysis method, and (3) to identify the dominant influential variables related to the cause of the observed trends in ETo in YRD.

2 Study area and data collection

2.1 Study area

The study area encompasses the region of the YRD in eastern China, located between approximately 27°01′ N and 35°20′ N and 114°54′ E and 123°08′ E (Fig. 1). The area is ca. 344,300 km^2 and includes Anhui province, Jiangsu province, Zhejiang province, and Shanghai municipality. The topography map in this region shows high elevation mainly in the south and west, and low elevation in the middle, east, and north. From the north to the south, the geomorphic types belong to the North China Plain, Yangtze River Plain, Jiangnan Hills, and Southeast Hills. The region has a typical East Asian monsoon climate, characterized by a hot wet summer and cold dry winter. The multiannual average precipitation decreases from southeast to northwest in general. The middle and north region is one of the most important grain production bases in China. The main crops here are rice, winter wheat, and maize. Irrigation water is needed the most in the spring and early summer months. Due to agricultural and industrial production, large numbers of surface water resources have been polluted. More serious for agricultural water demand is the excessive exploitation of underground water and extensive farming in the northern parts. At the same time, it is one of the most developed areas in China and also one of the largest urban agglomerations in the world. Intensive urbanization has changed the underlying surface significantly, which also changes the spatiotemporal patterns of ETo.

2.2 Data collection

Daily meteorological data of sufficient length from 46 stations in the research region were obtained from the National Meteorological Center of China (http://data.cma.gov.cn) from 1957 to 2014. The locations and elevations of these climatic stations are given in Fig. 1 and Table 1. The data included daily values of maximum air temperature (°C), minimum air temperature (°C), average air temperature (°C), sunshine duration (h), water vapor pressure (hPa), wind speed at a height of 10 m (m s^{-1}), and relative air humidity (%). For the

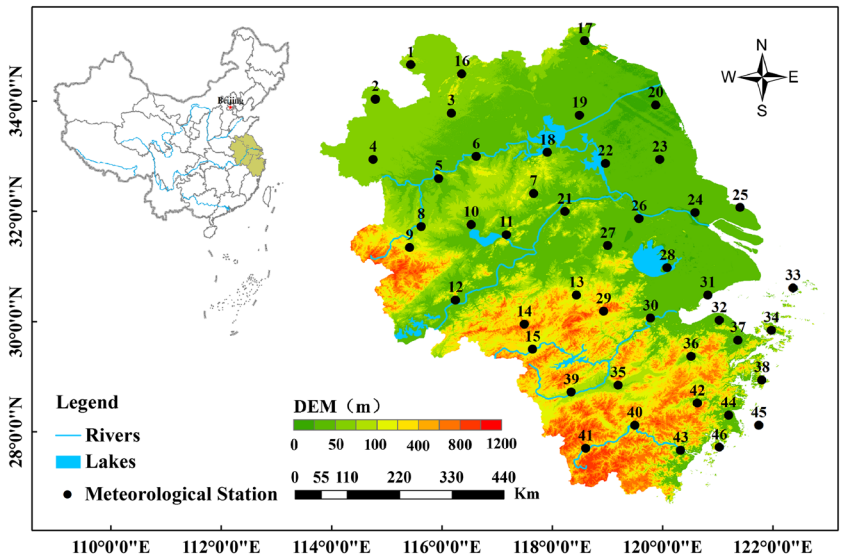

Fig. 1 Geographical location of the study region and meteorological stations

purpose of checking the quality of the data, we plotted the time series and visually inspected them for possible errors and missing data for all meteorological variables used in this study. We found that the missing data accounted for less than 0.3 % of the total data, and these were filled in using calculated data based on the neighboring stations through a simple linear regression method (Price et al. 2000). Also, Table 1 also shows the percentage of missing data for each meteorological station.

Table 1 Details of the meteorological stations in research region

Number	Station	Lat. (N)	Long. (E)	Elevation (m)	Missing data (%)	Number	Station	Lat. (N)	Long. (E)	Elevation (m)	Missing data (%)
1	Dangshan	34°26′	116°20′	44.2	0.27	24	Nantong	31°59′	120°53′	6.1	0.11
2	Bozhou	33°52′	115°46′	37.7	0.22	25	Lvsi	32°04′	121°36′	5.5	0.09
3	Suzhou	33°38′	116°59′	25.9	1.55	26	Changzhou	31°53′	119°59′	4.4	0.08
4	Fuyang	32°52′	115°44′	32.7	1.56	27	Liyang	31°26′	119°29′	7.7	0.06
5	Shouxian	32°33′	116°47′	22.7	0.58	28	Dongshan	31°04′	120°26′	17.5	0.14
6	Bengbu	32°55′	117°23′	21.9	0.26	29	Tianmushan	30°21′	119°25′	1505.9	0.04
7	Chuzhou	32°18′	118°18′	27.5	0	30	Hangzhou	30°14′	120°10′	41.7	0.03
8	Lu'an	31°45′	116°30′	60.5	0.43	31	Pinghu	30°37′	121°05′	5.4	0.06
9	Huoshan	31°24′	116°19′	86.4	0.46	32	Cixi	30°12′	121°16′	4.5	0.10
10	Hefei	31°47′	117°18′	27	0.40	33	Shengsi	30°44′	122°27′	79.6	0.14
11	Chaohu	31°37′	117°52′	22.4	0.31	34	Dinghai	30°02′	122°06′	35.7	0.09
12	Anqing	30°32′	117°03′	19.8	0.71	35	Jinhua	29°07′	119°39′	62.6	0.07
13	Ningguo	30°37′	118°59′	89.4	0.23	36	Shengzhou	29°36′	120°49′	104.3	0.03
14	Huangshan	30°08′	118°09′	1840.4	0.39	37	Yinxian	29°52′	121°34′	4.8	0.29
15	Tunxi	29°43′	118°17′	142.7	0	38	Shipu	29°12′	121°57′	128.4	0.04
16	Xuzhou	34°17′	117°09′	41.2	0.12	39	Quzhou	29°00′	118°54′	82.4	0.08
17	Ganyu	34°50′	119°07′	3.3	0.11	40	Lishui	28°27′	119°55′	59.7	0.24
18	Xuyi	32°59′	118°31′	40.8	0.08	41	Longquan	28°04′	119°08′	195.5	0.56
19	Huai'an	33°36′	119°02′	17.5	0.67	42	Kuocangshan	28°49′	120°55′	1383.1	0.04
20	Sheyang	33°46′	120°15′	2	0.01	43	Wenzhou	28°02′	120°39′	28.3	0.12
21	Nanjing	32°00′	118°48′	7.1	0.09	44	Hongjia	28°37′	121°25′	4.6	0.33
22	Gaoyou	32°48′	119°27′	5.4	1.08	45	Dachen	28°27′	121°54′	86.2	1.08
23	Dongtai	32°52′	120°19′	4.3	0.03	46	Yuhuan	28°05′	121°16′	95.9	0.13

3 Methodology

3.1 Calculation of ETo

Because of the difficulty of obtaining the accurate evapotranspiration, ETo was normally estimated. The conception of ETo was first introduced in the late 1970s and early 1980s to distinguish from potential evapotranspiration (Allen et al. 1998; Allen 2000). The term "Reference Crop Evapotranspiration" was defined as the rate of evapotranspiration from a hypothetical reference crop with an assumed crop height of 0.12 m, a fixed surface resistance of 70 s m^{-1}, and an albedo of 0.23, closely resembling the evapotranspiration from an extensive surface of green grass of uniform height, actively growing, well-watered, and completely shading the ground (Xu et al. 2006). There is a diversity of meteorological methods to calculate regional ETo, and the related data are mainly air temperature, wind speed, sunshine duration, and relative air humidity. Among those methods, daily or monthly average temperature is the only needed data for the simple ones, like the method proposed by Blaney et al. (1950). Generally, it seems that the result will be more accurate when more variables are being considered. FAO Penman-Monteith Method is widely accepted for calculating the ETo in different regions of the world, mainly because it is physically based on explicitly physical and aerodynamic parameters. The Penman-Monteith method can be derived as:

$$\mathrm{ET}_0 = \frac{0.408\Delta(R_\mathrm{n}-G) + r\dfrac{900}{T+273}u_2(e_\mathrm{s}-e_\mathrm{a})}{\Delta + r(1+0.34u_2)} \tag{1}$$

where ETo is the reference evapotranspiration (mm day^{-1}), Δ is the slope of vapor pressure curves (kPa $°C^{-1}$), R_n is the net radiation at the crop surface (MJ m^{-2} day^{-1}), γ is the psychrometric constant (kPa $°C^{-1}$), G is the soil heat flux density (MJ m^{-1} day^{-1}), T is the mean daily air temperature at 2 m height (°C), u_2 is the wind speed at 2 m height (m s^{-1}), e_s is the saturation of vapor pressure (kPa), and e_a is the actual vapor pressure (kPa). Because soil heat flux is smaller compared with R_n, and calculation time steps are 24 h, the estimation of G is assumed to be 0 in the ETo calculation. For this research region where no regional revisions of coefficients are available, the value of $a_\mathrm{s} = 0.25$ and $b_\mathrm{s} = 0.5$ that suggested by FAO were used to calculate the incoming and calculated solar radiation. The monthly and annual ETo has been calculated based on accumulation of daily values for a given month or year.

3.2 Modified Mann-Kendall trend test

The non-parametric Mann-Kendall trend test (Mann 1945; Kendall 1975) was selected to analyze the trend of ETo in this research, because it is distributed-free, robust against outliner, and has a higher power than many other commonly used tests. The Mann-Kendall trend test statistic S is calculated as:

$$S = \sum_{i=1}^{n-1}\sum_{j\neq i+1}^{n}\mathrm{sgn}(x_j - x_i) \tag{2}$$

where n is the number of data points, x_i and x_j are the data values in time series i and j ($j > i$), respectively, and $\mathrm{sgn}(x_j - x_i)$ is the sign function as:

$$\mathrm{sgn}(x_j - x_i) = \begin{cases} +1, \text{if } x_j - x_i > 0 \\ 0, \text{if } x_j - x_i = 0 \\ -1, \text{if } x_j - x_i < 0 \end{cases} \tag{3}$$

The variation is computed as:

$$\mathrm{Var}(S) = \frac{n(n-1)(2n+5) - \sum_{n-1}^{m} t_i(t_i-1)(2t_i+5)}{18} \tag{4}$$

where n is the number of data points, m is the number of tied groups, and t_i denotes the number of ties of extent i. A tied group is a set of sample data having the same values. In cases where the sample size $n > 10$, the standard normal test statistic Z_S is computed using Eq. (5):

$$Z_S = \begin{cases} \dfrac{S-1}{\sqrt{\mathrm{Var}(S)}}, \text{if S} > 0 \\ 0, \text{if S} = 0 \\ \dfrac{S+1}{\sqrt{\mathrm{Var}(S)}}, \text{if S} < 0 \end{cases} \tag{5}$$

$$P = 0.5 - \Phi(|Z|) \tag{6}$$

$$\Phi(|Z|) = \frac{1}{\sqrt{2\pi}}\int_0^{|Z|} e^{-\frac{t^2}{2}}dt \tag{7}$$

When $|Z_{1-\alpha/2}| > Z_\mathrm{S}$, the null hypothesis is rejected and a significant trend exists at the level of α in the time series. Otherwise, the null hypothesis of no trend was accepted. In this study, 95 % confidence level was used (Liang et al. 2010).

But Mann-Kendall trend test needs the sample data to be serially independent. When sample data are serially correlated, the result will be influenced. We use the Trend-Free Pre-Whitening (TFPW) approach developed by Yue and Wang (2004) to eliminate the effect of serial correlation on the Mann-Kendall test.

$$\beta = \mathrm{Median}\left(\frac{x_j - x_i}{j-i}\right)\forall i < j \tag{8}$$

$$Y_t = x_t - \beta t \tag{9}$$

$$r_1 = \frac{\sum_{t=1}^{n-1}\left(x_t - \overline{x}_t\right)\left(x_{t+1} - \overline{x}_{t+1}\right)}{\sqrt{\sum_{t=1}^{n-1}\left(x_t - \overline{x}_t\right)^2 \sum_{t=1}^{n-1}\left(x_{t+1} - \overline{x}_{t+1}\right)^2}} \quad (10)$$

$$r_1(\alpha = 0.1) = \frac{1 \pm 1.645\sqrt{n-2}}{n-1} \quad (11)$$

$$Y_t' = Y_t - r_1 Y_{t-1} \quad (12)$$

$$Y_t'' = Y_t' - \beta t \quad (13)$$

where x_i, x_j, x_t are the data values in time series i, j, and t; $\overline{x}_t$ and $\overline{x}_{t+1}$ are the mean data values in time series t and $t+1$. r_1 is the auto coefficient values of the first-order sequence.

3.3 Morlet wavelet analysis

Use the Morlet wavelet analysis method to explore the periodic variation of ETo in East China from 1957 to 2014. The wavelet function is calculated as follows:

$$\psi(t) = e^{ict} e^{-t^2/2} \quad (14)$$

where c is a constant and the value is 6.2; i is an imaginary number.

The wavelet transform coefficient formula is as follows:

$$W_f(a,b) = \left|a\right|^{-\frac{1}{2}} \int_{t=-\infty}^{\infty} f(x)\overline{\psi}\left(\frac{t-b}{a}\right) \mathrm{dt} = \left\langle f(x), \psi_{a,b}(t)\right\rangle \quad (15)$$

where $W_f(a, b)$ is the wavelet transform coefficients; $\psi(t)$ is the basic wavelet or mother wavelet; $\langle,\rangle$ is the inner product; a is the scale expansion factor; b is the time shift factor; $\psi_{a,b}(t)$ is the analysis wavelet or the continuous wavelet, and its formula is as follows:

$$\psi_{a,b}(t) = \left|a\right|^{-\frac{1}{2}} \psi\left(\frac{t-b}{a}\right), a, b \in R, a > 0 \quad (16)$$

The wavelet variance is computed as:

$$\mathrm{Var}(a) = \int_{-\infty}^{+\infty} \left|W_f(a,b)^2 \mathrm{db}\right| \quad (17)$$

3.4 Influence of climate variables on ETo change

In order to identify the main meteorological factors responsible for ETo variation in all station in research region, a multiple stepwise regression method was used between ETo series and seven meteorological factors (namely average air temperature, maximum air temperature, minimum air temperature, wind speed, sunshine duration, atmospheric pressure, and relative air humidity) (Chun et al. 2012; Cristea et al. 2012).

4 Results

4.1 Spatial and temporal distributions of annual and monthly ETo

4.1.1 Annual scale

Mean annual ETo over the study period at all meteorological stations was computed and is shown in Fig. 2. The results revealed that the average annual ETo was approximately 787.24 mm per year. The values varied from 523.78 to 959.75 mm per year between stations. Spatially, the areas with the highest ETo (mostly exceeding 860 mm) were mainly located in the northwest. This area is affected by dry continental air masses from the Mongolia Plateau, Siberia, and the Arctic Ocean, especially in winter and spring. The precipitation in eastern China is mainly from warm wet flow coming from the west Pacific Ocean. The retention of the rain belt is shorter than in the area in the south, leading to less rainfall, more sunshine days, and increased evapotranspiration. This causes severe problems as the region is one of the most important agricultural areas of China. In addition, the highest ETo values were also found in parts of the south, such as Anqing, Jinhua, and Quzhou. This is attributed to the local geomorphology, i.e., the low-lying basin and gorge area. Low-value zones were located in the southeast, especially in the high elevation areas such as Huangshan, Huoshan, Kuocangshan, and Tianmushan (Fig. 2).

4.1.2 Monthly scale

Figure 3 exhibits the distribution of average monthly ETo in all climatic stations in the YRD. The proportion of average monthly ETo ranges from 3.96 % (January) to 13.68 % (July).

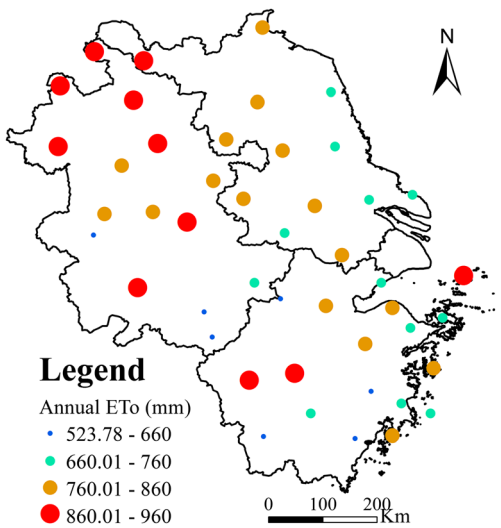

Fig. 2 Annual distribution of ETo

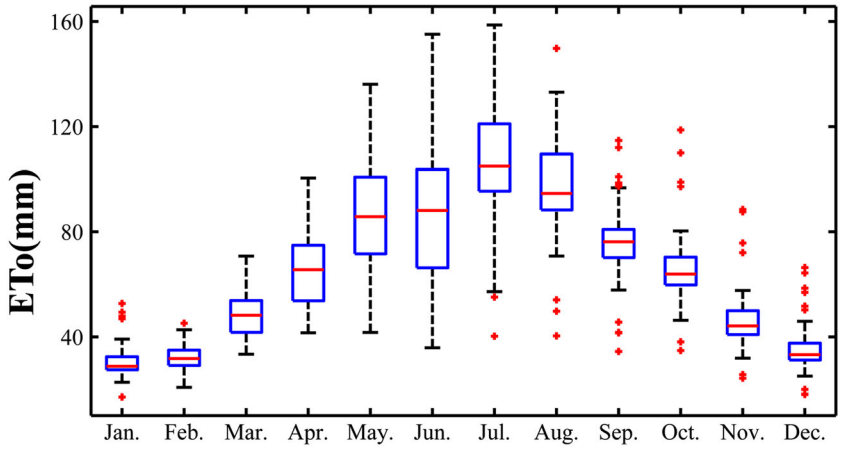

Fig. 3 Box and whisker plots of monthly ETo values

Average monthly ETo values rose and then declined, with July being the transition month. Additionally, the maximums, medians, and 75 % percentiles of monthly ETo values followed a similar temporal pattern in decline. However, for the minimums and 25 % percentiles, the gradual increasing trend was interrupted in June when the plum rain (the East Asian rainy season) prevailed in the study region. This reinforced an interesting phenomenon in which the variation in ETo values was the largest in the hot summer months and smallest in the cold winter months.

The spatial distribution of average monthly ETo in the research region varied (Fig. 4). From February to June, the local climate in the north was dominated by windy days and quickly increasing temperature, which are the main reasons for higher values of ETo. The highest average monthly ETo rose rapidly and continuously from 45.20 mm in February to 155.13 mm in June. In the southern area, coastal locations and higher elevations caused the relatively cold and humid conditions and thus lower ETo values. In July and August, things changed. The high ETo values were located in the middle and southern areas due to the summer drought. At the same time, the rain belt from the west Pacific Ocean reached the northern area. From September onwards, with the activation of dry and cold air masses from the Mongolian Plateau and Siberia, temperature in the YRD decreased rapidly, as well as the ETo. In autumn and winter, the higher ETo values mainly emerged in the southeast coastal region and islands.

Due to the influence of ETo on agricultural production, the spatial distribution of monthly ETo in the YRD will have a significant negative effect on crops. In the northern area, winter wheat is the most important crop, and water resources are under high demand during the growth stages of elongation, earing, flowering, grouting, and maturing from April to June, when the ETo is the most intensive and increasing rapidly. In the southern area, the rice-growing period stretches from May to October, and the vegetation period of rice suffers an intensive ETo of over 100 mm per month in the summer drought period.

4.2 Spatial and temporal trends of annual and monthly ETo

4.2.1 Temporal trends in ETo

In order to detect the temporal changes of the annual ETo in the study region, linear regression analysis was carried out. The analysis shows an overall positive trend with a change of 22.51 mm every decade during the period from 1957 to 2014 (Fig. 5a). The positive trend was also verified by modified Mann-Kendall trend test with Z values reaching 3.76. In order to avoid the error influenced by persistence effects of the time series, the ETo series were modified by TFPW method. Annual ETo in the last 58 years fluctuated widely, decreasing at first and then increasing, with the transition period in the late 1980s and early 1990s. The year of change in annual ETo is 1999, i.e., the increase in annual ETo from 1957 to 2014 began around 1999 (Fig. 5b). Figure 5c maps the Morlet wavelet analysis results for annual average ETo. The variance shows that there are several wavelet periods in different stages. Within a confidence level of 95 %, the 2–3-year cycle exists from the 1970s to the first half of the 1990s. From the late 1990s to the first half of the 2000s, the regression cycle is around to 3–4 years. At the same time, 9- and 15-year cycles of annual ETo are concentrated in the 1970s–1990s and 1980s–2000s.

Changes in ETo were investigated by the modified Mann-Kendall trend test at the annual and monthly scale at all meteorological stations, and the results of

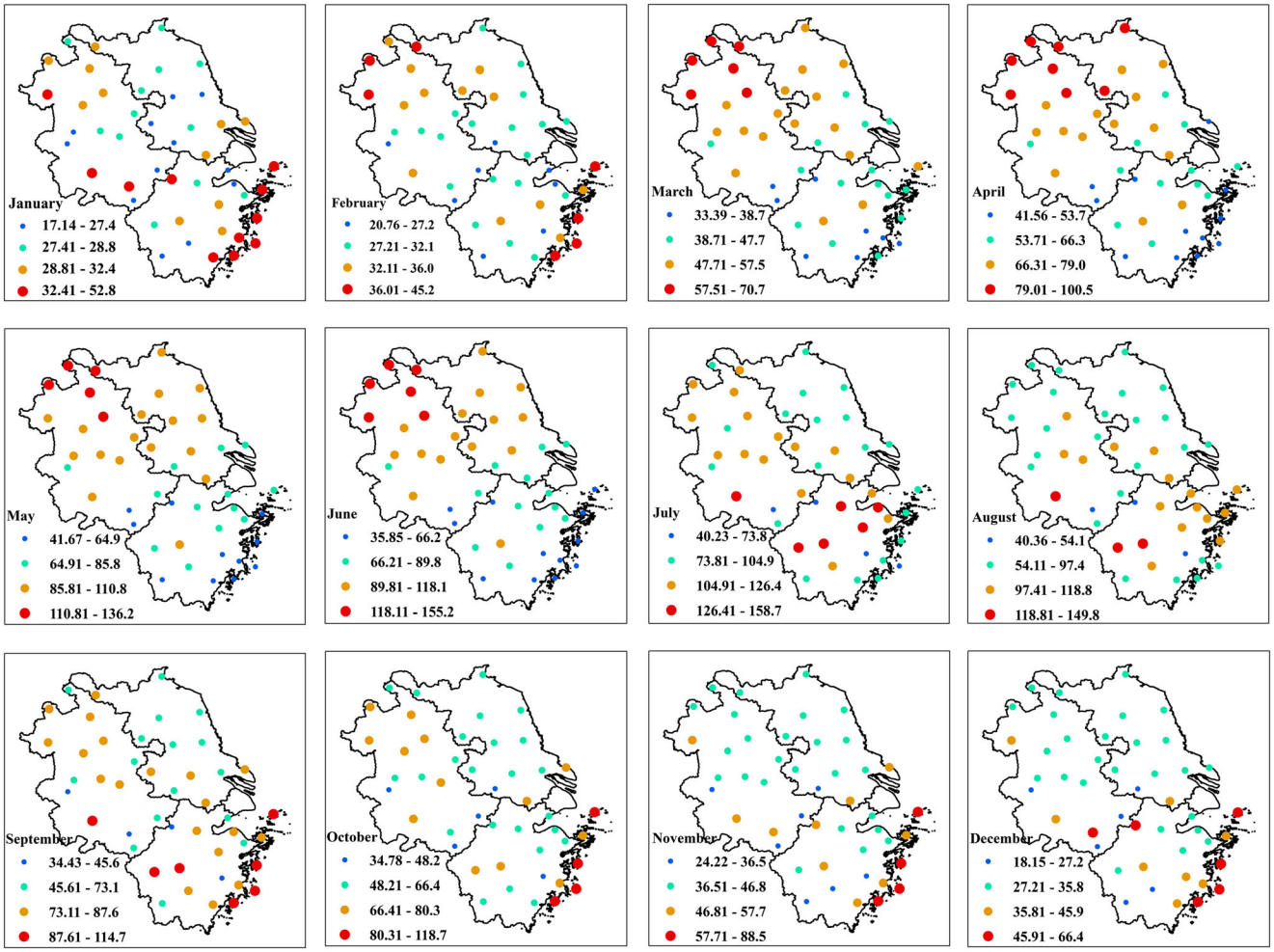

Fig. 4 Monthly distribution of ETo

ETo trends are shown in Table 2. At the annual scale, both positive and negative trends were observed, 73.9 and 26.1 %, respectively. Increasing and decreasing trends showing statistical significance occurred in 26.1 and 15.2 % of stations, respectively. At the monthly scale, the number of stations with positive trends was no less than that of negative trends except in January, February, and August. The most widespread increase was detected in April at the proportion of 95.7 %.

Figure 6 shows the box plot of Z values, calculated through the modified Mann-Kendall trend test for annual and monthly ETo time series at all meteorological stations. At the annual scale, an increasing trend was found in about three-quarters of stations, as illustrated by the 25 % percentile that is located above the zero line of Z values. At the monthly scale, the median of Z values is located above the zero line except for January and August. The maximum Z value (6.06) was observed in September, whereas the minimum value (−3.55) was in January. It is interesting to note that there is no significant decrease from February to May.

4.2.2 Spatial trends in ETo

Figure 7 shows the spatial distribution of annual ETo calculated by the modified Mann-Kendall trend test in the YRD from 1957 to 2014. The map shows that both positive and negative trends were observed in different weather stations. A significant increase in ETo values was dominant in the eastern and southeastern area. In this region, the underlying surface changed profoundly due to economic development since the reform and the opening-up policies formulated in China. The climate also changed in the subsequent chain reaction. Combined with a significant decrease in annual precipitation in eastern China, water shortages became more serious.

At the same time, only 12 stations (26.09 % of the total) showed a decrease in ETo, mostly in the northern area. A significant decrease in ETo was reported in only 5 stations, 4 of which are located in the northern area. This area is one of the main agricultural production regions in China, and is located in the transition zone of humid to semiarid climate.

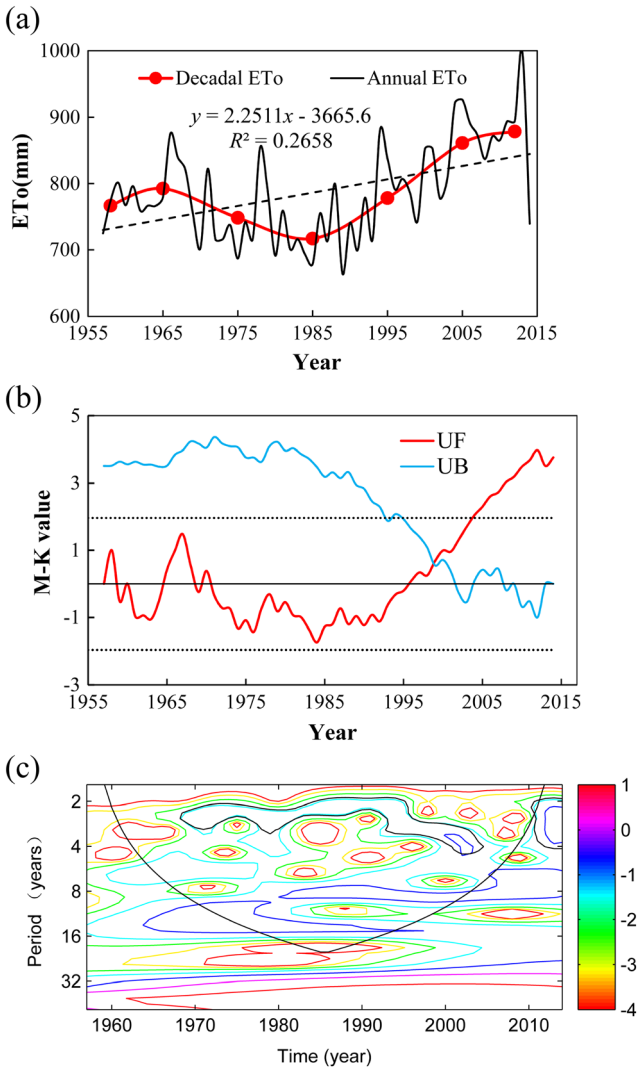

Fig. 5 **a** Linear regression analysis. **b** Mann-Kendall test. **c** Morlet wavelet analysis results for annual average ETo

Decreasing ETo will reduce the pressure on water resources to a certain degree for agricultural and social development.

Monthly analysis shows that January is the month with the most numerous weather stations recording decreasing ETo, but the decrease is rarely significant (Fig. 8). The stations with a significant decrease in ETo are mainly located in the northern and eastern areas. A significant increase in ETo happened only in the Hongjia climatic station (location 44), located in the southeastern part. More stations exhibit a decrease rather than an increase in ETo in February, but there were no significant decreasing trends. The intensive increasing trend mainly appeared in the southeastern part.

However, in spring (March, April, and May), most meteorological stations experienced a significant increase in ETo, which enhanced the frequency and intensity of drought with seasonal precipitation less than average. The significant increase was found in almost all the research regions in the southeast. At the same time, detected changes also included decreasing trends in some meteorological stations in the northern area. During the summer months (June, July, and August), the increasing trend of ETo weakened and was mainly detected in the eastern coastal area, while the significant decreasing trend was also identified in the northwestern area. At the other times of the year, both increasing and decreasing trends existed but increasing trends dominated, and the spatial distribution was similar to that in the spring months. What is more, the decreasing trends appeared not only in the north but also in the southeast area in November.

Based on the previous analysis, decreasing trends in annual ETo in the northern area seem to be the combined effect of decreasing trends in monthly ETo values in January, February, June, August, September, October, and December. Increasing trends of ETo values were also detected in a minority of climatic stations in the northern area in some other months, but this did not influence the regional annual trend. In the eastern and southeastern parts, the increasing annual ETo is due to the occurrence of increasing ETo in most months, especially in the spring and autumn months. Similar increasing trends in annual ETo in the western area were also contributed to by the spring and autumn months.

4.2.3 Stage difference in ETo

According to the previous research results in this study, when considering the period 1957 to 2014, annual ETo values had a major transition period in the late 1980s and early 1990s. The study period was divided into two stages: 1957–1989 (stage I) and 1990–2014 (stage II). Compared with stage I, annual

Table 2 Frequencies of different trend-types in annual and monthly scales obtained through Mann-Kendall trend test (%)

Trend	Jan.	Feb.	Mar.	Apr.	May	Jun.	Jul.	Aug.	Sep.	Oct.	Nov.	Dec.	Ann.
Positive	26.1	50.0	91.1	95.7	88.9	58.7	69.6	47.8	79.5	82.6	69.6	76.1	73.9
Positive (Sig.)	23.9	41.3	46.7	26.1	17.8	43.5	56.5	41.3	40.9	39.1	45.7	52.2	26.1
Negative	73.9	50.0	8.9	4.3	11.1	41.3	30.4	52.2	20.5	17.4	30.4	23.9	26.1
Negative (Sig.)	58.7	50.0	6.7	4.3	8.9	32.6	26.1	34.8	18.2	13.0	26.1	23.9	15.2

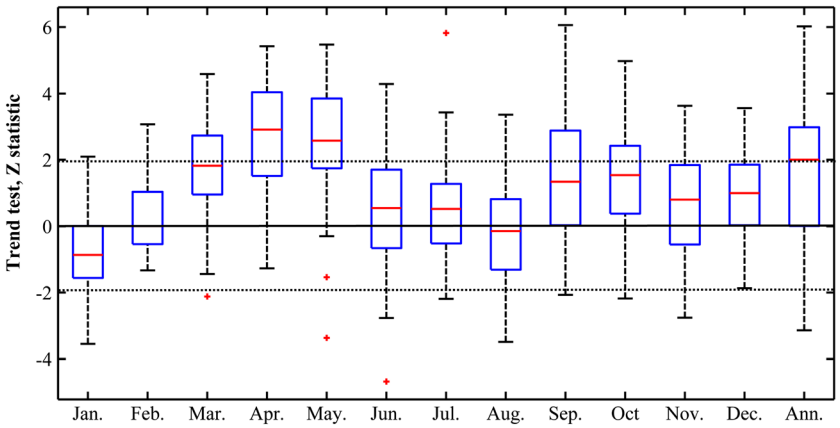

Fig. 6 Box and whisker plots of monthly ETo trends, *Z* values, obtained through the modified Mann-Kendall trend test among meteorological

average ETo values in the later stage were higher in most weather stations. The spatial distribution of difference between the two stages is shown in Fig. 9. In the middle and southeastern areas, the ETo values increased more than 100 mm. At the same time, decreasing trends were mainly located in the northern and southern areas.

The difference between the two stages is not only the average annual ETo values, but also a change in trends. According to Table 3, more than half of the meteorological stations had statistically significant decreasing trends in annual ETo values during stage I. In addition, almost 85 % of stations witnessed decreasing trends. At a monthly scale, the change styles can be summarized into four types: (1) similar to annual pattern, happened in July; (2) decreasing but insignificant, happened in January, February, March, June, August, September, and October; (3) numbers of increasing and decreasing trends close to equal in May and November; and (4) increasing trends dominated in April and December.

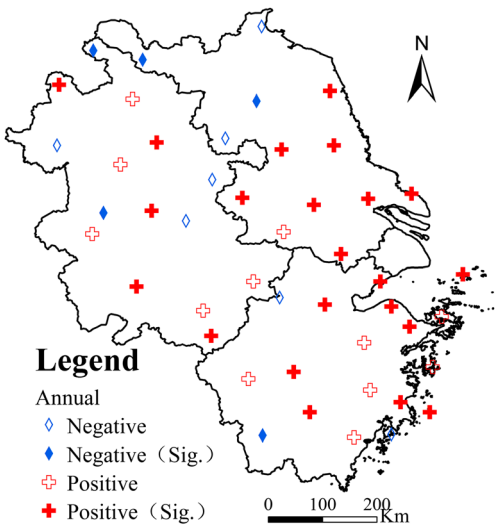

Fig. 7 Annual trends of ETo over the period of 1957–2014

During stage II, great changes occurred (Table 3). At the annual timescale, more than half of the stations presented significant increasing trends. At the monthly scale, increasing trends were also dominant except in February and September, when decreasing trends accounted for more than 50 % (including significant and insignificant decreasing trends).

4.3 Variables influencing annual ETo

In order to detect the variables influencing ETo, we computed the changes in the basic climatic parameters: air temperature, wind speed, sunshine duration, relative humidity, and atmospheric pressure. A summary of the results is presented in Table 4. Increases in average air temperature, maximum air temperature, and minimum air temperature were detected in over 80 % of the meteorological stations since 1957, and most of them were found to be statistically significant at the 95 % level. However, average wind speed, annual sunshine duration, atmospheric pressure, and relative humidity decreased in the majority of stations.

Due to human activities and natural development, climate at the earth's surface has changed a lot in recent years, and ETo has changed accordingly. For further study, the dominant meteorological factors affecting the ETo trends were analyzed using a multivariate regression model in 46 stations at an annual timescale (Fig. 10). Relative humidity was found to be the most important variable influencing annual ETo (i.e., 32 out of 46 stations, almost 70 %), especially in coastal areas. At the same time, average wind speed was the most important variable in some areas of the northwest and southwest. The annual ETo in the stations of Shouxian and Changzhou was affected by maximum air temperature and average air temperature, respectively. From Table 5, average wind speed, followed by sunshine duration, was detected to be the most important influencing factor.

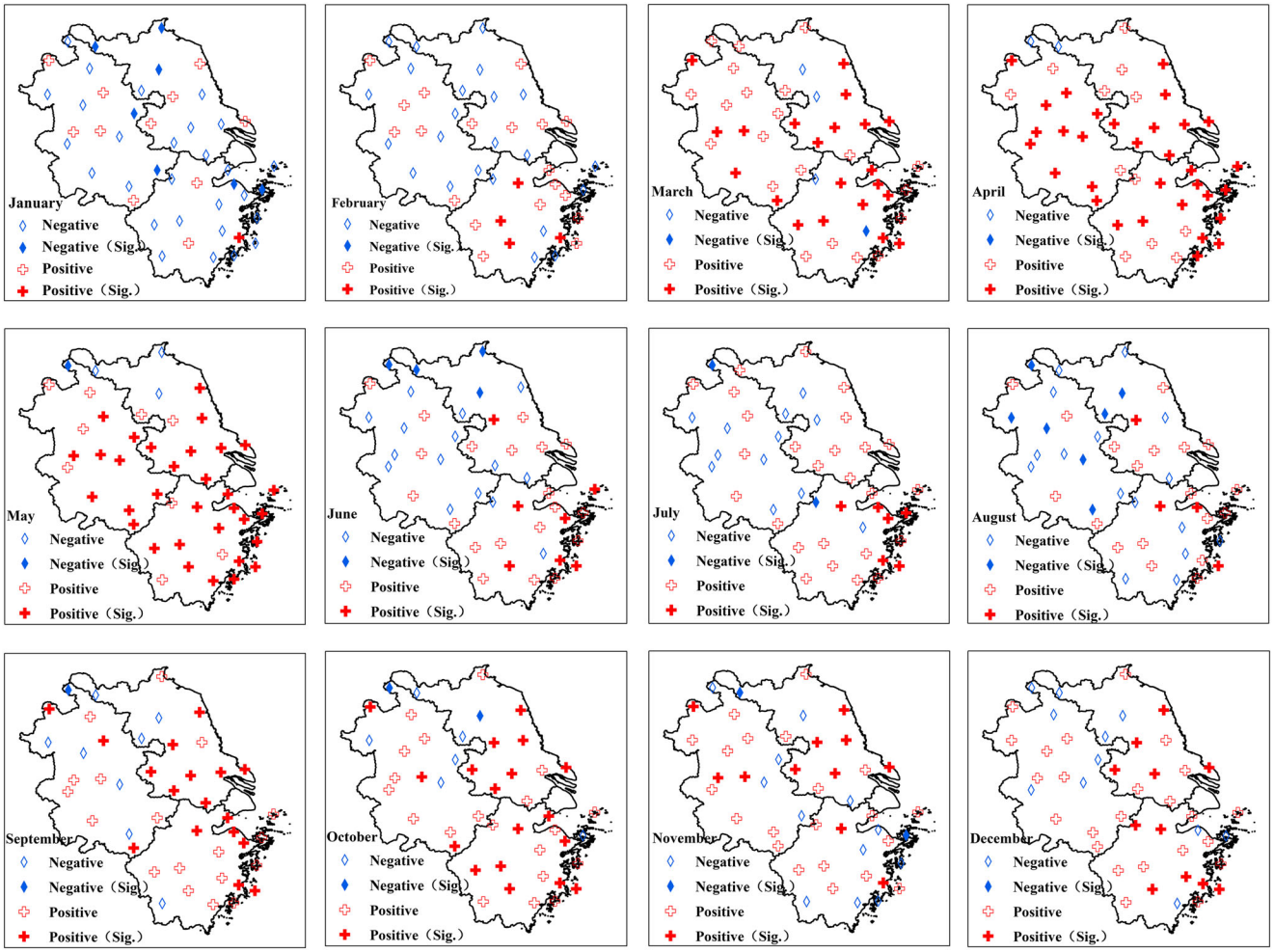

Fig. 8 Monthly trends of ETo over the period of 1957–2014

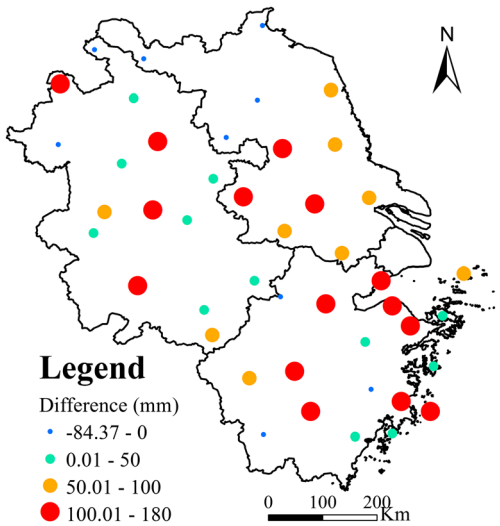

Fig. 9 Spatial distribution on difference of average ETo between the periods of 1957–1989

5 Discussion

5.1 ETo distribution

Spatial distribution of average annual ETo has been observed to be the highest in tropical and semi-tropical arid areas (Lawrimore and Peterson 2000; Burn and Hesch 2007; Roderick et al. 2007; Bandyopadhayay et al. 2009; Dinpashoh et al. 2011; Nam et al. 2015). On the other hand, low-value zones were always found in the cold areas, especially the high elevation areas and near polar regions. In China, studies have shown that the distribution of average annual ETo is similar to that in other regions of the world. The annual average ETo values in northwestern China were around 1100–1400 mm but no more than 800 mm in the Sichuan Basin, northern northeast China, and the eastern Tibetan plateau (Gao et al. 2006). At a seasonal or monthly timescale, spatial patterns may be very different at an annual scale, mainly attributed to the changing weather systems within the year. So, when we explore the spatial patterns of ETo

Table 3 Frequencies of annual and monthly changes in annual and monthly ETo values in different stages (%)

Stage	Trend style	Jan.	Feb.	Mar.	Apr.	May	Jun.	Jul.	Aug.	Sep.	Oct.	Nov.	Dec.	Ann.
Stage I	Significant upward	0	0	0	8.7	6.5	0	2.2	0	2.2	2.2	8.7	19.6	4.4
	Insignificant upward	10.9	15.2	15.2	69.6	45.7	19.6	8.7	13.0	10.9	23.9	47.8	60.9	10.9
	Significant downward	26.1	6.5	26.1	4.4	2.2	21.7	56.5	32.6	30.4	15.2	0	0	54.4
	Insignificant downward	63.0	78.3	58.7	17.4	45.7	58.7	32.6	54.4	56.5	58.7	43.5	19.6	30.4
Stage II	Significant upward	26.2	2.4	80.5	53.7	40.5	12.2	26.8	21.4	19.5	33.3	14.3	36.6	51.2
	Insignificant upward	64.3	12.2	19.5	43.9	47.6	61.0	43.9	54.8	29.3	38.1	45.2	51.2	32.6
	Significant downward	0	22.0	0	2.4	2.4	2.4	0	4.8	22.0	7.1	7.1	0	2.3
	Insignificant downward	9.5	63.4	0	0	9.5	24.4	29.3	19.1	29.3	21.4	33.3	12.2	14.0

values, the geographic and atmospheric factors should be given sufficient consideration.

5.2 ETo trend

Based on the modified Mann-Kendall trend test, both increasing and decreasing trends of annual and monthly ETo were detected in different parts of the research region. Increasing trends in ETo were normally found in the eastern and southeastern areas, and decreasing trends were concentrated in the northern region. In recent years, similar studies have shown that annual ETo values exhibited significant decreasing trends for China as a whole (Yin et al. 2010). But the trends have an obvious regional difference: decreasing trends mainly emerged in northern China, southwestern China, and northwestern China, whereas increasing trends were located in parts of northern northeast China, central China, and southern China (Liu and Yang 2010; Liu et al. 2010; Wang et al. 2011; Ma et al. 2012; Tang et al. 2011; Yang et al. 2013). Such results are in accordance with our findings. In spite of this, duration of time series is another important factor that should be taken into account when we are trying to detect the changing trend of ETo. Gao et al. (2006) analyzed potential evapotranspiration over China from 1956 to 2000 by using the Penman-Monteith method and found decreasing trends of annual ETo in the whole of east China, except for parts of northeastern China. At the same time, she also found that the transition of the ETo trend happened in the 1980s. But when we lengthen the time series to 2014, the overall trend will be the opposite in most meteorological stations.

5.3 Impact of meteorological variables to ETo trend

Many earlier scientists were devoted to the topic of influential variables on ETo in China. Thomas (2000) and Yin et al. (2010) reported that sunshine duration, followed by wind speed, is the main parameter that affected annual ETo in south China; however, wind speed and relative humidity are the most important climatic variables in northwestern and mid-eastern China, respectively. Shan et al. (2015) detected that at an annual timescale, the negative trend of ETo was dominated by decreasing wind speed and increasing air temperature in the Beijing-Tianjin Sand Source Control Project Region. The pan evaporation of the Yangtze River was mostly influenced by wind speed and relative humidity, but the main factors influencing evapotranspiration in this region were net total radiation, relative humidity, air temperature, and wind speed (Xu et al. 2006).

Similar situations have also been found in other parts of the world. Bandyopadhayay et al. (2009) detected that relative humidity and wind speed are the two main climatic factors responsible for ETo change. Goyal (2004) found that temperature, radiation, wind speed, and vapor pressure all influence the ETo a lot. Wind speed, followed by relative humidity, was

Table 4 Annual changes in main climate parameters (% of the total number of data series considered) in the period of 1957–2014

Trend type	*T*	Tmax	Tmin	Wn	Sn	Pr	Hu	ETo
Significant increasing	95.6	80.4	95.6	0	0	17.4	0	26.1
Insignificant increasing	2.2	17.4	4.4	6.5	2.2	17.4	10.9	47.8
Significant decreasing	0	0	0	80.4	91.3	45.6	76.1	10.9
Insignificant decreasing	2.2	2.2	0	13.1	6.5	19.6	13.0	15.2

T average air temperature, *Tmax* maximum air temperature, *Tmin* minimum air temperature, *Wn* wind speed, *Sn* sunshine duration, *Pr* atmospheric pressure, *Hu* relative air humidity

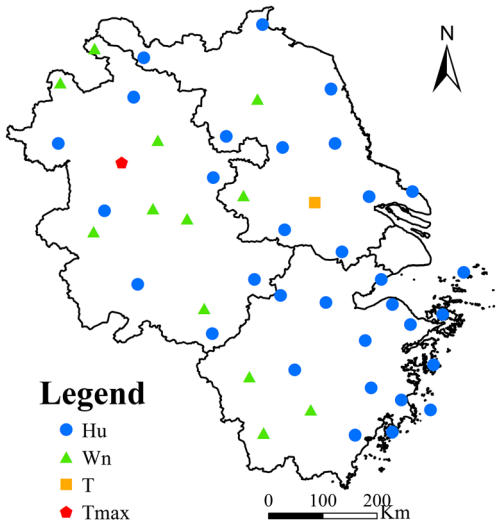

Fig. 10 Spatial distribution of dominant variables to annual ETo trends during 1957 to 2014

the most important meteorological factor affecting ETo in Iran (Dinpashoh et al. 2011).

Many scientists are trying to explain why evapotranspiration has decreased in so many parts of the world while there is global warming, especially in mid-latitude regions including Europe, America, Australia, as well as China. The major reason is that higher air temperature leads to more powerful atmospheric water holding capacity, resulting in an increase of cloud cover and decrease of solar radiation reaching the earth's surface. However, cloud cover has decreased due to aggregated aerosols and pollution from energy consumption (Ren et al. 2005; Streets et al. 2008). Goyal (2004) even announced that a 1 % increase in temperature could lead to a 15-mm increase in evapotranspiration.

In other words, there has been no agreement about the relationship between climate change and evapotranspiration change until now. Besides global warming, human activities could also exert an important influence on ETo change. Terrestrial ecosystems, potential vegetation restoration, and deforestation will change the level of small particulate matter in the atmosphere, and regional climate factors such as precipitation, relative humidity, and wind speed, will eventually impact the regional ETo. Agricultural activities will also contribute to the interactions between earth surface and atmosphere. Ozdogan and Roderick have paid attention to the impact of large-scale irrigation on regional evapotranspiration (Ozdogan and Salvucci 2004; Roderick and Farquhar 2004). Special attention should be paid to identifying the impacts of human activities and the interaction among different variables on ETo change to improve our understanding of ETo change.

In order to further detect ETo change, we should make the relationship among different climatic factors clear, and take the mutual influences of so many factors into account.

Table 5 Times of meteorological variables affects annual ETo the most, second, and third

	T	Tmax	Tmin	Wn	Sn	P	Hu
First	2.2	2.2	0	26.1	0	0	69.6
Second	2.2	2.2	8.7	30.4	28.3	2.2	26.1
Third	17.4	26.1	17.4	6.5	21.7	8.7	2.2

6 Conclusion

Due to the importance of detecting regional crop water demand and hydrological circulation, ETo at 46 meteorological stations in the YRD, eastern China, was calculated using the Penman-Monteith method based on daily data of climatic variables from 1957 to 2014. The temporal distribution was identified based on the Mann-Kendall trend test, linear regression, and wavelet analysis. Furthermore, the influential variables were detected by a multiple stepwise regression method.

The results showed that the spatial distribution of higher average annual ETo values in the northwest reached 900 mm, and were lower in the south. The lowest values were mainly located in high elevation areas. A similar distribution happened from February to June, whereas the opposite situation was identified in July and August. In the remaining months of the year, high values were concentrated in coastal areas. A broad pattern of regional annual ETo trend was detected with an increase of 22.51 mm per decade in YRD. Annual ETo values increased in approximately 74 % of meteorological stations. The minority of meteorological stations with a decreasing trend were mainly in the northern areas. At a monthly scale, the number of stations with positive trends was no less than that of negative trends except in January, February, and August. The most intensive and dominant increasing trends were identified in March, April, and May.

Furthermore, a transition period appeared in the late 1980s and early 1990s, dividing the series into two stages, with decreasing and increasing trends, respectively. The annual and monthly ETo values showed a mainly decreasing trend except in April, May, November, and December during stage I. Nevertheless, there was an increasing trend in more than 50 % of the meteorological stations in stage II, except in February and September.

Relative humidity was the most important meteorological element influencing annual ETo change, followed by wind speed and sunshine duration. The increasing trends of annual ETo in most climatic stations were the combined influence of decreasing relative humidity, wind speed, sunshine duration, and increasing average air temperature, maximum air temperature, and minimum air temperature.

Acknowledgments This research was funded by the National Key Research and Development Plan of China (No. 2016YFC0401502), National Natural Science Foundation of China (No. 41371046), Commonweal and Specialized Program for Scientific Research, Ministry of Water Resources of China (No. 201201072), the Natural Science Foundation of Jiangsu Province (No. BK20131276), and the Water Conservancy Science Foundation of Jiangsu Province (No. 2015003). Thanks to the National Meteorological Information Center, China Meteorological Administration for offering the meteorological data. The authors would like to thank the two anonymous reviews and editor for their constructive criticism and valuable comments to improve the quality of the manuscript.

References

Allen RG (2000) REF-ET, reference evapotranspiration calculator version Windows 2.0. User's manual. University of Idaho Research and Extension Center, Kimberly, ID

Allen RG, Pereira LS, Raes D, Smith M (1998) Crop evapotranspiration: guideline for computing crop water requirement. FAO irrigation and drainage paper no. 56. Food and Agriculture Organization, Italy

Bandyopadhayay A, Bhadra A, Raghuwanshi NS, Singh R (2009) Temporal trends in estimates of reference evapotranspiration over India. J Hydrol Eng 14(5):508–518

Blaney HP, Criddle WD, Blaney HF, et al. (1950) Determining water requirements in irrigated areas from climatological and irrigation data. In: Tech Paper 96. USDA Soil of Conservation Service. The Conterminous United States. Colorado State University, Fort Collins, CO

Burn DH, Hesch NM (2007) Trends in evaporation for the Canadian prairies. J Hydrol 336(1–2):61–73

Chen X, Liu X, Zhou G, Han L, Liu W, Liao J (2015) 50-year evapotranspiration declining and potential causations in subtropical Guangdong province, southern China. Catena 128:185–194

Chi Y, Zhang C, Liang C, Wu H (2013) The precipitation changes in eastern forest regions of China in recent 50 years. Acta Ecol Sin 33:217–226

Chun KP, Wheater HS, Onof C (2012) Projecting and hind casting potential evaporation for the UK between 1950 and 2099. Clim Chang 113:639–661

Cristea NC, Kampf SK, Burges SJ (2012) Linear models for estimating annual and growing season reference evapotranspiration using averages of weather variables. Int J Climatol 33(2):376–387

Croitoru AE, Piticar A, Dragota CS, Burada DC (2013) Recent changes in reference evapotranspiration in Romania. Glob Planet Chang 111: 127–132

Dinpashoh Y, Jhajharia D, Fajheri-Fard A, Singh VP, Kahya E (2011) Trends in reference crop evapotranspiration over Iran. J Hydro 399: 422–433. doi:10.1016/j.jhydrol.2011.01.021

Feng J, Yan D, Li C, Yu F, Zhang C (2014) Assessing the impact of climatic factors on potential evapotranspiration in droughts in North China. Quatern Int 336:6–12

Gao G, Chen D, Ren G, et al. (2006) Trend of potential evapotranspiration over China during 1956 to 2000. Geographic Res 25(3):378–387 in Chinese

Goyal RK (2004) Sensitivity of evapotranspiration to global warming: a case study of arid zone of Rajasthan (India. Agric Water Manag 69(1):1–11

Jhajharia D, Shrivastava SK, Sarkar D, Sarkar S (2009) Temporal characteristics of pan evaporation trends under the humid conditions of northeast India. Agric For Meteorol 149:763–770

Jones DA, Wang W, Fawcett R (2009) High-quality spatial climate datasets for Australia. Aust Meteorol Ocean 58(4):233–248

Kendall MG (1975) Rank correlation methods. Griffin, London

Lawrimore JH, Peterson TC (2000) Pan evaporation trend in dry and humid regions of the United States. J Hydrometeorol 1(6):543–546

Liang LQ, Li LJ, Liu Q (2010) Temporal variation of reference evapotranspiration during 1961-2005 in the Taoer River basin of Northeast China. Agric For Meteorol 150(2):298–306

Lins HF, Slack JR (2005) Seasonal and regional characteristics of US stream flow trends in the United States from 1940 to 1999. Phys Geogr 26(6):489–501

Liu Q, Yang Z (2010) Quantitative estimation of the impact of climate change on actual evapotranspiration in the Yellow River Basin, China. J Hydrol 395:226–234

Liu Q, Yang Z, Cui B, Sun T (2010) The temporal trends of reference evapotranspiration and its sensitivity to key meteorological variables in the Yellow River Basin, China. Hydrol Process 24(15):2171–2181

Ma XN, Zhang MJ, Li YJ, Wang SJ, Ma Q, Liu WL (2012) Decreasing potential evapotranspiration in the Huanghe River watershed in climate warming during 1960–2010. J Geogr Sci 22(6):977–988

Mann HB (1945) Nonparametric tests against trend. Econometrica 13(3): 245–259

Monteith JL (1965) Evaporation and environment. Symp Soc for Exp Biol 19:205–234

Nam W, Hong E, Choi J (2015) Has climate change already affected the spatial distribution and temporal trends of reference evapotranspiration in South Korea? Agric Water Manag 150:129–138

Ozdogan M, Salvucci GD (2004) Irrigation-induced changes in potential evapotranspiration in southeastern Turkey: test and application of Boucher's complementary hypothesis. Water Resour Res 40(4). doi:10.1029/2003WR002822

Penman HL (1948) Natural evaporation from open water, bare soil and grass. Proc R Soc Lond 193:120–145

Price DT, McKenny DW, Nalder IA, Hutchinson MF, Kesteven JL (2000) A comparison of two statistical methods for spatial interpolation of Canadian monthly mean climate data. Agric For Meteorol 101:81–94

Priestley CH, Taylor RJ (1972) On the assessment of surface heat flux and evaporation using larger-scale parameters. Mon Weather Rev 100(2):81–92

Ren GY, Guo J, Xu ZM, Chu ZY, Zhang L, Zou XK, Li QX, Liu XN (2005) Climate change of China's mainland over the last half century. Acta Meterol Sin 63:942–956 in Chinese

Roderick ML, Farquhar GD (2004) Changes in Australian pan evaporation from 1970 to 2002. Int J Climatol 24(9):1077–1090

Roderick ML, Rostayn LD, Farquhar GD, Hobbins MT (2007) On the attribution of changing pan evaporation. Geophys Res Lett 34(17): 403. doi:10.1029/2007GL031166

Sahoo D, Smith PK (2009) Hydro climatic trend detection in a rapidly urbanizing semi-arid and coastal river basin. J Hydrol 367:217–224

Shan N, Shi Z, Yang X, Gao J, Cai D (2015) Spatiotemporal trends of reference evapotranspiration and its driving factors in the Beijing–Tianjin Sand Source Control Project Region, China. Agric For Meteorol 200:322–333. doi:10.1016/j.agrformet.2014.10.008

Streets DG, Yu C, Wu Y, Chin M, Zhao ZC, Hayasaka T, Shi GY (2008) Aerosol trends over China, 1980–2000. Atmos Res 88(2):174–182

Tang B, Tong L, Kang SZ, Zhang L (2011) Impacts of climate variability on reference evapotranspiration over 58 years in the Haihe river basin of North China. Agric Water Manag 98:1660–1670

Tayanc M, Karaca M, Yenigun O (1997) Annual and seasonal air temperature trend patterns of climate change and urbanization effects in relation to air pollutants in Turkey. J Geophys Res 102(D2):1909–1919

Thomas A (2000) Spatial and temporal characteristics of potential evapotranspiration trends over China. Int J Climatol 20:381–396

Thornthwaite CW (1948) An approach toward a rational classification of climate. Geographic Rev 38:55–94

Wang W, Peng S, Yang T, Shao Q, Xu J, Xing W (2011) Spatial and temporal characteristics of reference evapotranspiration trends in the Haihe River basin, China. J Hydrol Eng 16(3):239–252

Xu CY, Gong LB, Jiang T, Chen DL, Singh VP (2006) Analysis of spatial distribution and temporal trend of reference evapotranspiration and pan evaporation in Changjiang (Yangtze River) catchment. J Hydrol 327:81–93

Yang Y, Zhang Z, Xiang X (2009) Spatial variation of reference crop evapotranspiration on Tibetan Plateau. Water. Sci Eng 2(1):112–120

Yang JY, Liu Q, Mei XR, Yan CR, Ju H, Xue JW (2013) Spatiotemporal characteristics of reference evapotranspiration and its sensitivity coefficients to climate factors in Huang-Huai-Hai Plain, China. J Integr Agric 12(12):2280–2291

Yin YH, Wu SH, Dai EF (2010) Determining factors in potential evapotranspiration changes over China in the period 1971–2008. Chin Sci Bull 55(29):3329–3337. doi:10.1007/s11434-010-3289-y

Yue S, Wang C (2004) The Mann-Kendall test modified by effective sample size to detect trend in serially correlated hydrological series. Water Resources Manag 18:201–218

Zhang X, Harvey KD, Hogg WD, Yuzyk TR (2001) Trends in Canadian stream flow. Water Resources Res 37(4):987–998

Zhang X, Kang S, Zhang L, Liu J (2010) Spatial variations of climatology monthly crop reference evapotranspiration and sensitivity coefficients in Shiyang river basin of northwest China. Agr. Water Manage 97:1506–1516

Zhang Q, Xu C, Chen X (2011a) Reference evapotranspiration changes in China: natural processes or human influences? Theor Appl Climatol 103:479–488

Zhang Q, Xu C, Chen YD, Ren L (2011b) Comparison of evapotranspiration variations between the Yellow River and Pearl River basin, China. Stoch Environ Res Risk Assess 25:139–150

Zhang Q, Qi T, Li J, Singh VP, Wang Z (2015) Spatiotemporal variations of pan evaporation in China during 1960–2005: changing patterns and causes. Int J Climatol 35:903–912

Zhao Y, Zou X, Zhang J, Cao L, Xu X, Zhang K, Chen Y (2014) Spatiotemporal variation of reference evapotranspiration and aridity index in the Loess Plateau Region of China, during 1961-2012. Quatern. Int. 349:196–206